Monitoring forest cover change within different reserve types in southern Ghana

Yu Hsin Tsai ⬤ · Douglas A. Stow · David López-Carr ·
John R. Weeks · Keith C. Clarke · Foster Mensah

Abstract Rapid population and economic growth quickly degrade and deplete forest resources in many developing countries, even within protected areas. Monitoring forest cover change is critical for assessing ecosystem changes and targeting conservation efforts. Yet the most biodiverse forests on the planet are also the most difficult to monitor remotely due to their frequent cloud cover. To begin to reconcile this problem, we develop and implement an effective and efficient approach to mapping forest loss in the extremely cloud-prevalent southern Ghana region using dense time series Landsat 7 and 8 images from 1999 to 2018, based on median value temporal compositing of a novel vegetation index called the spectral variability vegetation index (SVVI). Resultant land-cover and land-use maps yielded 90 to 94% mapping accuracies. Our results indicate 625 km^2 of forest loss within the 9800-km^2 total mapping area, including within forest reserves and their environs between circa 2003 and 2018. Within the reserves, reduced forest cover is found near the reserve boundaries compared with their interiors, suggesting a more degraded environment near the edge of the protected areas. A fully protected reserve, Kakum National Park, showed little forest cover change compared with many other less protected reserves (such as a production reserve—Subri River). Anthropogenic activities, such as mining, agriculture, and built area expansion, were the main land-use transitions from forest. The reserves and census districts that are located near large-scale open pit mining indicated the most drastic forest loss. No significant correlation was found between the magnitudes of forest cover change and population density change for reserves and within a 1.5-km buffer surrounding the reserves. While other anthropogenic factors should be explored in relation to deforestation, our qualitative analysis revealed that reserve protection status (management policies) appears to be an important factor. The mapping approach described in this study provided a highly accurate and effective means to monitor land-use changes in forested and cloud-prone regions with great promise for application to improved monitoring of moist tropical and other forests characterized by high cloud cover.

Y. H. Tsai (✉) · D. A. Stow · J. R. Weeks
Department of Geography, San Diego State University, San Diego, CA, USA
e-mail: cindyxtsai@gmail.com

D. López-Carr · K. C. Clarke
Department of Geography, University of California, Santa Barbara, CA, USA

F. Mensah
Center for Remote Sensing and Geographical Information Services, Accra, Ghana

Introduction

Forest cover is associated with ecosystem services that are vital to human health and livelihoods, including watershed protection, climate change mitigation, and soil erosion prevention. However, tropical forests globally were depleted at an annual rate of 6 million hectares in recent years, while agricultural land increased by almost the same amount, based on a report by the Food and Agriculture Organization of the United Nations (FAO 2016). Other studies indicate that most of the deforestation in tropical forests is related to agricultural practices (Barraclough and Ghimire 2000; Appiah et al. 2009; UNEP GEO-5 report 2012). Population dynamics (such as birth, death, and migration) have also been commonly associated as an underlying and indirect cause for deforestation, particularly in rural regions (Carr 2004; Carr et al. 2005). Ghana, as a developing country in sub-Saharan Africa, has experienced steady economic, population, and urban growth, and in turn, land-cover and land-use change (Acheampong et al. 2018). The country's total population increased from 19 million to 25 million between 2000 and 2010 (Ghana Statistical Service 2012). Ghana's GDP had an annual gain of 6.6% from 2010 to 2014 (FAO 2016). Despite the net rural-to-urban migration and over half of the population residing in urban areas since 2010, the rural population continues to grow, suggesting that fertility rates remain high (UN DESA 2018).

Forest resources and deforestation in Ghana

Most of the pristine forest resources, including tropical evergreen seasonal forest and tropical semi-deciduous forest (UNESCO 1973), are located in the high forest zone in the southern part of Ghana. Historically, these primary forests in Ghana are mostly depleted due to past agricultural expansion and over-exploitation of forest resources (Appiah et al. 2009). Timber harvesting, surface mining, and export-oriented agriculture are among the main economic activities in Ghana (Hens and Boon 1999; UN DESA 2017), and these activities are destructive to forest cover (Osafo 2005). Heavy logging took place during the 1960s and 70s in Ghana. Almost all forests, even within protected areas, have been selectively logged at some point in time, many of them since 1990. Vegetation outside of the reserves is mostly secondary regeneration on abandoned farms (Hall and Swaine 1976; Dickson et al. 1988), with small

agricultural plots mixed in. Expansions of plantations of trees, oil palm, and cocoa also contribute to deforestation or forest degradation. The commonly practiced taungya system, in which plantation workers are given rights to grow agriculture crops among forest plantations, can cause forest disturbances (Kalame et al. 2011; Hawthorne and Abu-Juam 1995). Unsuccessful taungya systems can lead to forest cover conversion to agriculture; this "slash-and-burn" agriculture practice can also lead to higher fire risk within plantations and forests. Ghana is a major producer of gold, bauxite, and manganese among African countries. In 2016, its total gold output was over 113,400 kg. Twenty-three large-scale mines were located in the country in 2016, and most of them operate as open pit mines. This surface mining style and mine expansions cause both large- and small-scale forest cover removal.

It is estimated by the FAO that the livelihood of 2.5 million people in Ghana depends on forests. Appiah et al. (2009) documented that almost 40% of rural household income in Ghana consists of forest-related activities. More revenue is generated and more forest is cleared when the household is larger or resides closer to forests. With a lack of off-farm work opportunities, rural residents rely on poverty-driven agriculture (compared with economical, longer-cycle planting). Short cycle crops are planted and shifted between agriculture plots while long cycle crops are also cultivated. This practice generates higher crop yields but is also destructive to forest cover (Barraclough and Ghimire 2000). Firewood collection from fields and forest near villages is also common in rural regions (Calvo 1994). Firewood is the preferred and main fuel source for cooking in rural zones, and few households use charcoal or crop residue according to the Ghana 2010 population and household census (Ghana Statistical Service 2012). Due to deforestation, the travel time and distance to collect firewood have increased in recent years according to a UN report (2010).

Individuals and local communities/tribes own roughly 80% of the lands in Ghana. Most of these customary lands are managed based on indigenous tribal customary laws and are not bound by specific national management laws (Ubink and Quan 2008). Some of these customary lands, such as sacred groves and community forests, are preserved as areas for traditional shrines for local communities. The remaining 20% of lands in Ghana are state owned, which the Ghanaian government owns and manages. Over 200 forest reserves and

protected areas (i.e., on-reserves) are set aside to be managed by the Ghanaian government (Osafo 2005), and they are located on both customary land and state land. However, reserves are further classified with different protection status and human disturbances are still present. Protected areas are classified as conversion, production, and protected reserves (Hilson and Nyame 2006). Conversion reserves are degraded regions that are being targeted for replanting. Production reserves are resource reserves that can be used to sustainably produce wildlife products, and timber and non-timber products, used for cultural practices (e.g., tribal sacred lands), tourism, and trophy hunting (Hawthorne and Abu-Juam 1995). Protected reserves, including national parks, allow no exploitation. However, based on a management evaluation report published by the International Union for Conservation of Nature (Hawthorne and Abu-Juam 1995), even protected reserves and national parks can experience land conversion, bush fire, and encroachment.

Remote sensing solutions to monitoring land change in cloud-prone areas

Remote sensing offers a cost-effective and practical means to map vegetation, other land-cover, and land-use over large areas, compared with field survey. Moderate spatial resolution satellite systems such as Landsat provide near-global coverage of multi-spectral imagery dating back to the mid-1980s that can be used to monitor long-term and extensive forest cover (Roy et al. 2014). Landsat surface reflectance products offer more comparable and reliable land change analysis than spectral radiance or digital number products (Hall et al. 1991; Moran et al. 1992) as the conversion accounts for some atmospheric and solar illumination effects. These surface reflectance products are generated by algorithms implemented by the Landsat Ecosystem Disturbance Adaptive Processing System (LEDAPS; Masek et al. 2006) for Landsat 4 to 7 imagery, and Landsat Surface Reflectance Code (LaSRC; Vermote et al. 2016) for Landsat 8 images.

Optical satellite imagery is susceptible to cloud cover, particularly in humid and tropical regions where cloud cover and optically dense atmospheres are predominant. Much research has demonstrated the potential of image composites, formed by combining multi-temporal cloud-free observations, to resolve cloud cover and cloud shadow issues (Broich et al. 2011; Huang

et al. 2009; Hansen et al. 2008). Lindquist et al. (2008) evaluated the pixel quality for the humid tropics in central Africa and found that, ideally, all available image data would be utilized to achieve the highest image composite quality. Coulter et al. (2016) used dense Landsat images to derive maximum-value image composites as a means to resolve the frequent cloud cover and cloud shadow issue in southern Ghana. Their derived land-cover and land-use change map detected changes with over 70% accuracy, although some image anomalies from maximum-value compositing were present. Ruefenacht (2016) tested the utility of median value image composites to estimating tree canopy percent cover. Median value composites were found to retain comparable image information and yielded fewer image anomalies from the cloud and shadow pixels compared with the maximum-value composite products, as median value is more resistant to data outliers. The utility of median value image composites is demonstrated in this study of southern Ghana.

Unsupervised image classification or clustering followed by manual labelling is commonly adopted for large area land-cover mapping, particularly when the mapping classes are uncomplicated (Franklin and Wulder 2002) or when training data are not readily available for supervised image classifiers (Rogan and Chen 2004). Muller et al. (1999) mapped vegetation in northern Alaska spanning multiple scenes of Landsat images using K-means clustering. Forest and meadow were discriminated using the Landsat imagery and ISODATA clustering in Yellowstone by Debinski et al. (1999). Unsupervised image classification techniques have also been applied to map land-cover and land-use in Ghana. Pabi (2007) used Landsat TM images and ISODATA clustering to map land-cover and land-use for eight sites within two census districts in central Ghana. With a post-classification map comparison between 1991 and 2001, Pabi found that dense woodland areas decreased significantly in all eight sites while cultivated land increased. The effectiveness of unsupervised image classification has not yet been tested in mapping the extensive tropical southern Ghana region where cloud cover is prevalent.

Land-cover and land-use change in Ghana has been examined in previous studies based on remote sensing data and techniques, mostly for localized areas. Forest cover decrease and concomitant increase in other land-uses (e.g., built, agriculture, and mining area) are common findings in these studies. Kusimi (2008) mapped

land-cover and land-use change for 1986–2002 within a single census district in southwestern Ghana, using Landsat TM images and a combination of unsupervised and supervised image classification routines. He found that forest reserves in the district experienced significant forest cover loss of over 400 km^2, while areas of mining, farming, built, and settlements in the district increased. Yorke and Margai (2007) mapped land-cover and land-use from 1990 to 2000 Landsat images using a supervised, maximum likelihood image classification routine for a watershed in southeastern Ghana. They found forest cover decreased by over 32%, while agricultural land and built land expanded substantially. Coulter et al. (2016) mapped land-cover changes between circa 2000 and 2010 using four Landsat scenes covering much of southern Ghana, and found that 62% of the land changes were related to agricultural land increase. An up-to-date and more extensive examination of forest cover change in southern Ghana is needed and can aid in land-use decisions and conservation efforts.

The objectives of this study are twofold. First, land-cover and land-use changes with an emphasis on forest cover change for protected areas and their environs in southern Ghana are mapped and quantified based on Landsat multi-temporal composite data. Second, the magnitude of forest loss in relation to population growth between 2000 and 2010 is examined. Forest cover and other land-cover and land-use types are mapped for two study periods from 1999 to 2018. Changes in forest cover are quantified and examined in conjunction with high spatial resolution satellite images to identify the corresponding causes of land change. A regression analysis is utilized to evaluate the potential anthropogenic pressure on forest cover by examining the statistical relationship between forest loss and population growth.

Study area and data

Figure 1 shows the protected areas and forest reserves in the Western, Ashanti, Eastern, and Central regions of Ghana that were selected for this study. The selected 76 reserves are located in the tropical evergreen forest zone and within a single Landsat image scene. Among the selected reserves is a fully protected reserve, Kakum National Park. Kakum National Park is located in the Central region in Ghana. Established in 1931, Kakum National Park is currently being considered as a

UNESCO World Heritage Site for its high biodiversity and esthetic value. Kakum National Park covers a total of 212 km^2. Poaching has been identified as one of the main wildlife threats in this area (Hawthorne and Abu-Juam 1995). Farming activities surrounding the park are key deforestation drivers. Subri River, the largest reserve in Ghana (588 km^2) is a production reserve in the study area. Other production reserves are included as well, such as Opon Mansi and Bowiye Range. Reserves that are near some of the largest open pit mines in Ghana are also included (e.g., Bonsa Ben, Oda River, Anwhiaso, and Wassaw Conservation Areas). Many potential anthropogenic disturbances exist in these protected areas besides mining, including villages located at the reserve boundaries, large-scale commercial agriculture, and logging exploitation. Based on the average one-way walking time for firewood collection in rural Ghana (Calvo 1994; United Nations 2010), a 1.5-km surrounding area of each reserve is incorporated in addition to the reserve lands as the mapping area for this study, as seen in Fig. 1. Based on a polygon shapefile of protected areas provided by the Forestry Commission of Ghana, a subset and buffer of the reserves were created to delineate the mapping area. The total designated reserve area in this study is about 5370 km^2, and the total mapping area (i.e., reserves and environs) is about 9800 km^2.

Surface reflectance image products located at Worldwide Reference System 2 path 194 and row 56 collected from the Landsat 4 and 5 Thematic Mapper (TM), Landsat 7 Enhanced Thematic Mapper Plus (ETM+), and Landsat 8 Operational Land Imager (OLI) platforms were reviewed interactively on the Google Earth Engine platform (earthengine.google.com) and in the USGS Earth Explorer (earthexplorer.usgs.gov). The imagery data were limited to only Landsat Tier-1 surface reflectance products, for they meet certain radiometric and geometric standards during processing to ensure a consistent data quality that supports multi-temporal image analysis (Hall et al. 1991; Moran et al. 1992; USGS landsat.usgs.gov/landsat-level-1-standard-data-products). Based on image and reference data availability, two compositing periods were selected for this study—circa 2003 and circa 2018. The circa 2003 composite image was generated from all available Landsat 7 ETM+ image scenes (i.e., 39 scenes total) captured from January 1999 to mid-May of 2003. The circa 2018 composite image consists of multi-spectral data from all available Landsat 8 OLI images (i.e., 41
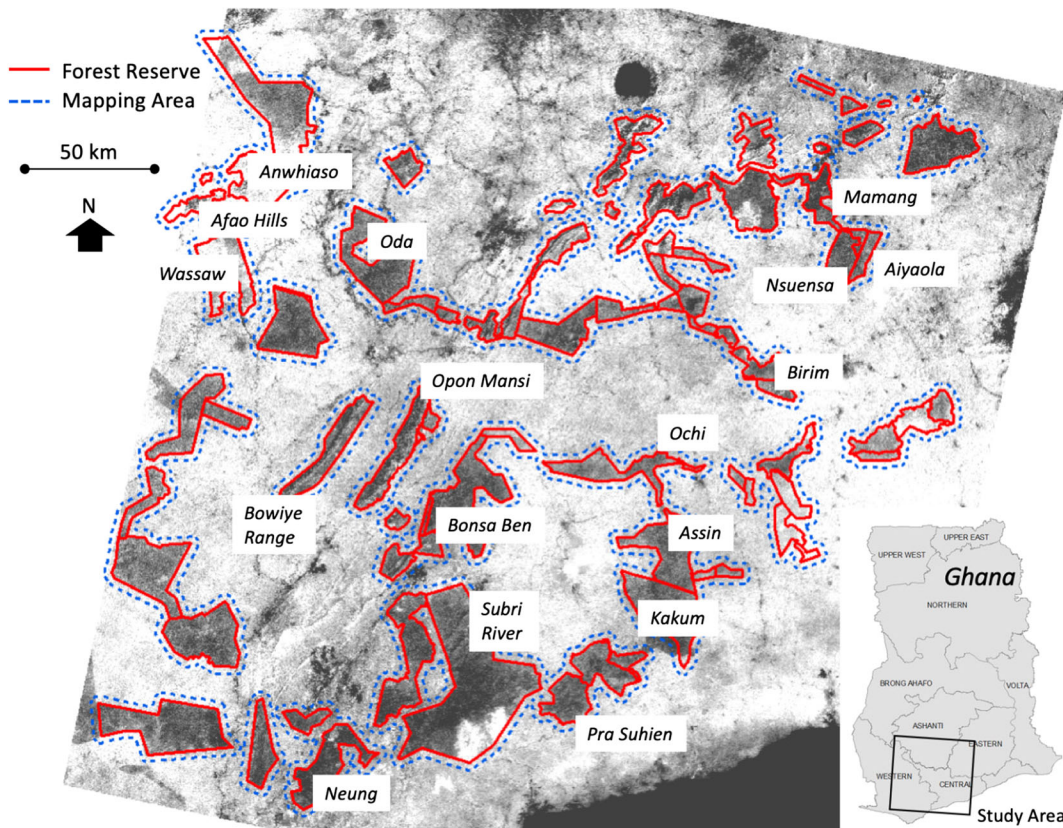
Fig. 1 Study area map showing forest reserves (outlined in red) and the mapping area (blue) in southern Ghana. Reserves are located in Western, Central, Eastern, and Ashanti regions. The gray-scale base image is the NIR band of a Landsat 8 OLI image captured in December 2015

scenes) collected between January 2013 and May 2018. We experimented with circa 1991 (using Landsat 4 and 5 TM images) and 2010 (using Landsat 7 ETM+ images) image composites for this study. Only six Landsat TM images are available for the study area due to a lack of a data recording station between 1986 and 1991 prior to the launch of Landsat 7 in 1999. Likely due to the limited number of images in the composite and lower image quality, the circa 1991 composite image yielded a problematic land-cover map with a lower mapping accuracy. Landsat 7 images collected after mid-May 2003 were affected by the Scan Line Corrector issue (i.e., SLC-off) for the ETM+ sensor. The post-2003 Landsat 7 images were not considered in this study after we found the dense forest regions susceptible to scan line data gaps.

Some high spatial resolution satellite imagery collected in recent years for southern Ghana was available as reference data. QuickBird and IKONOS images were available for viewing on Google Earth. WorldView-2 and a Digital Globe high spatial resolution commercial satellite image mosaic (collected between 2012 and 2014) is available for viewing as the BaseMap Imagery product in ArcGIS software. Three-meter spatial resolution planet imageries collected in Fall 2017 and Spring 2018 are also available through the Planet Education and Research program (Planet Team 2017). Three relatively cloud-free Landsat images were identified and downloaded from Earth Explorer for visual interpretation. The images corresponding to the study periods were collected in May 2002 (Landsat 7), December 2015, and January 2018 (both Landsat 8).

Methods

Landsat surface reflectance products were retrieved from the Google Earth Engine image library and processed using its JavaScript-based code editor platform. The images were masked for clouds, cloud shadow, and

water bodies using the pixel quality assessment band (i.e., pixel_qa) that was derived by the C version of the Function of Mask algorithm (CFMask; Foga et al. 2017) and provided as part of the Landsat surface reflectance products. A reflectance normalization process developed by Wu (2004) was applied to the Landsat surface reflectance images to correct for terrain effects. Each spectral band was divided by the sum of all spectral bands for each image date to minimize the illumination differences. The illumination normalized data were used for the subsequent image analysis.

Median value image composites were formed using the available cloud-free pixels for the study periods. Besides the Landsat spectral bands, spectral variability vegetation index (SVVI) and a SVVI texture image were also generated. SVVI was developed through exploratory analysis in a previous study mapping land-cover and land-use in southern Ghana (Coulter et al. 2016). It is calculated as the difference between the standard deviation (SD) of all Landsat spectral bands and the standard deviation of infrared bands for a given pixel, as defined in Eq. 1:

$$SVVI = SD(\rho_{all\ bands}) - SD(\rho_{NIR\ and\ SWIR\ bands}) \qquad (1)$$

Here, $\rho_{all\ bands}$ and $\rho_{NIR\ and\ SWIR\ bands}$ represent surface reflectance values for all Landsat bands (excluding thermal) and near-infrared and shortwave-infrared reflectance values respectively, for a given pixel. The SVVI metric was found to effectively minimize image compositing artifacts and to enhance the spectral and textural difference between natural vegetation and subsistence agriculture land in the southern Ghana study area.

SVVI was calculated for each image date captured within the study periods and composited using the median value for each pixel within the dense time stack. Forest and moist natural vegetation exhibits a low SVVI value, compared with non-vegetated areas, and shows low variability among the surrounding pixels. Thus, texture images were generated based on the SVVI products, calculated with a 3-by-3 focal standard deviation function to further differentiate forest and other non-forested land-cover types. A SVVI texture composite image was subsequently created using the median pixel values of the entire time series.

The median value composite layers of red and near-infrared spectral bands, SVVI, and SVVI texture were layer-stacked and utilized as the land-cover classification input. An unsupervised image classifier using K-means clustering was used to classify the images. Five hundred image pixels within the mapping area were randomly selected as the image classifier training data. Spectral clusters were generated by the K-means image classifier while the number of clusters was experimented on iteratively. The cluster images were examined in conjunction with high spatial resolution reference imagery and relatively cloud-free single-date Landsat imagery for the corresponding study period. Image clusters were merged and assigned manually into three classes: forest, agriculture/open canopy, and built/bare/surface mining. The forest class represents the undisturbed dense forest, mostly seen as closed canopy forest cover. The agriculture and open canopy class includes sparse secondary forest regeneration, oil palm/cocoa plantations, low-intensity subsistence agriculture, and fallow land. The built, bare, and mining class includes built-up, roads, cleared land with exposed soil, and surface mining. After the image classification, a 3-by-3 focal mode smoothing function was applied to the Landsat-derived maps to yield a generalized map at a more appropriate minimum mapping unit (closer to 1 ha) and to reduce per-pixel classification noise.

Classification accuracies were assessed using a total of 120 reference image pixels. The reference pixels were generated in a stratified random sampling manner and interpreted in conjunction with available high spatial resolution reference imagery and relatively cloud-free Landsat images to identify the corresponding land-cover and land-use types. Forty samples for each of the three mapping classes—forest, agriculture/open canopy, and built/mining—were created and reviewed to ensure the reference pixels represented stable and single class land-cover and land-use types during circa 2003 to 2018. The resulting reference pixels were used to measure the mapping accuracy of each study period. The mapping agreement, user's, producer's, and overall accuracies were summarized in an accuracy assessment table.

Land-cover and land-use change maps were generated based on the multi-temporal Landsat-derived map products through post-classification map comparison. Spatial patterns of forest loss (e.g., locations where closed forest transitioned to non-forest classes) were examined both quantitatively and qualitatively. Areal data of forest loss was summarized at the reserve and census district levels. Districts are relatively large census units, composed of multiple enumeration areas (similar to census blocks in the US), and each district

encompasses multiple forest reserves. Areal summaries of reserves were aggregated to the district level prior to analysis. Only districts that contained 15% or greater amounts of reserved land were selected for analysis. There are 14 districts within the study area that meet the 15% areal threshold.

Regression analyses were carried out to examine the amount of forest loss in relation to population density and population density change. Forest cover change was summarized for circa 2003–2018. Population data were derived from the decadal Ghana Population and Housing Census (PHC) from the years 2000 to 2010. The PHC data are georeferenced to the Enumeration Area (EA) level. The population density of EAs that are within a 1.5-km distance from the reserve boundary was averaged for each reserve. The population density was also summarized to the census district level and compared with the forest cover change amounts within each district. Two other independent variables (i.e., cooking fuel types and occupations) were also examined but the data variance was too limited to enable statistical analyses.

Results

Land-cover and land-use maps for circa 2003 and 2018 are shown in Fig. 2. The circa 2018 images generated using K-means clustering were based on 25 spectral clusters while the circa 2003 image was created with 16 spectral clusters. Mapping accuracies for the Landsat-derived maps are shown in Table 1. High overall mapping accuracies were achieved for both study periods, with the overall classification accuracies at 94 and 90% for circa 2003 and 2018, respectively. As Table 1 shows, some confusion occurred between the forest and open canopy vegetation classes, with slight confusion between built and open canopy vegetation for both image dates. The forest class appears to be over-classified for both study periods, as the user's accuracies are slightly lower than the producer's accuracies. The open canopy/agriculture class on the other hand is under-classified, with higher user's accuracies compared with producer's accuracies. The built/mining class is mapped with high accuracy, with nearly 100% producer's and user's accuracies for both dates.

As seen in Fig. 2, the dense evergreen forest cover is generally constrained within reserve boundaries. Open canopy and agriculture are mostly found outside of reserves. Some small patches of forest were mapped beyond reserve boundaries, mixed in with agriculture and open canopy. Unpaved roads inside reserves, forest clearing, and regeneration were also classified as open canopy. Built and surface mining are found near and within reserves. Some changes in forest cover and non-forest vegetation are apparent from the Landsat-derived classification products. About 80 km^2 of forest clearing is identified in Subri River forest reserve in the south of the mapping area between 2003 and 2018. The Anwhiaso East reserve located in the northeastern portion of the mapping area also shows forest loss during this period. Expansion in built and mining land-uses is also observed, particularly on the western side of the study area. Roads within reserve lands increased or at least became more definable in the Landsat images captured during the 2003 to 2018 period.

Table 2 summarizes areal land-cover and land-use and change between the two image periods for the entire mapping area (i.e., almost 9800 km^2), which varies slightly between image dates and data coverage. The percent areal change is calculated as the relative change, which is the difference between the two mapping dates relative to the earlier date. A total of 6655 km^2 or 68% of the mapping area was mapped as forest cover in circa 2003. The forest cover decreased by -625 km^2 or -9% between circa 2003 and 2018. The open canopy and agricultural land exhibit the opposite temporal dynamics, with an increase of over 535 km^2 (18% relative increase) since circa 2003. Built, bare, and surface mining showed a consistent increase in area, with a doubling of area since circa 2003.

Figure 3 shows the land-cover and land-use change map between circa 2003 and 2018 for the study area. Most of the reserve land remained dense forest canopy between circa 2003 and 2018, about 5142 km^2 in area. Almost 1500 km^2 of forest in circa 2003 transitioned to open canopy or agriculture land in circa 2018 (shown in blue in Fig. 3), mostly in the western portion of the study area. Over 2000 km^2 of land remained open canopy or agricultural land during this period, most of which was outside the protected area boundaries. Besides road network expansion through the forest reserves creating linear patterns of forest loss, logging, mining, and agricultural development contributed to most of the large-scale forest conversion. Over 110 km^2 was mapped as built and mining expansion (from both forest and agriculture/open canopy are in yellow and red,

Fig. 2 Land-cover and land-use maps for circa 2003 (top) and circa 2018 (bottom). The mapping area includes forest reserves and a 1.5-km outward buffer region from reserve boundaries. The background is a gray-scale NIR Landsat 8 image from December 2015
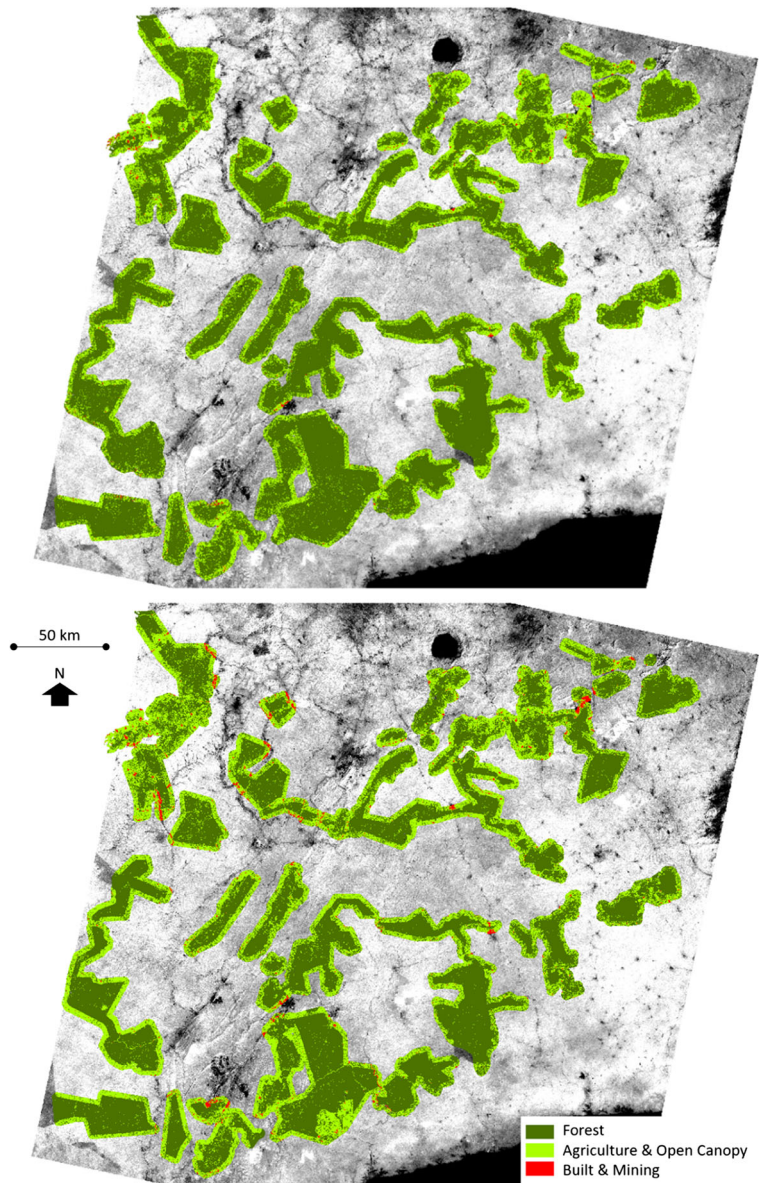
respectively, in Fig. 3). Large groupings of new built land and mining occurred in the northwest, northeast, and south in portions of the mapping area. Mining expansion is observed within the reserves northwest of the study area in the circa 2003 to 2018 period.

Forest cover within the reserve boundaries is observed to be more fragmented and declined near reserve boundaries in Figs. 2 and 3. Forest cover was quantified based on inward buffer zones from reserve boundaries to evaluate edge effects (Murcia 1995). An areal summary is given in Table 3.

Forest cover and forest cover change both exhibited substantial fragmentation and reduction near the reserve boundaries. Forest cover increased from 88 to 93% in circa 2003 moving from reserve boundaries to the interior of the reserves. The proportion of forest for circa 2018 exhibited a similar pattern but with a lower proportion compared with 2003. The 2018 forest cover showed a gradual increase from 82 to 90% as the distance inward from reserve boundaries increases. Areas within 500 m of reserve boundaries showed the greatest forest to non-forest transition between circa 2003 and

Table 1 Mapping accuracies of the Landsat-derived classification products for circa 2003 and 2018. The accuracies were evaluated using 40 reference pixels per class, 120 pixels total for each study period

Image-derived class	Reference class						User's accuracy %	
	Forest		Open canopy		Built			
	2003	2018	2003	2018	2003	2018	2003	2018
Forest	*39*	*37*	5	8			89	82
Open canopy	1	3	*35*	*32*	1	1	95	89
Built					*39*	*39*	100	100
Producer's accuracy %	98	93	88	80	98	98	Overall accuracy %	
							94	90

2018. A 13% relative forest loss from 2003 to 2018 is observed within this 500-m buffer zone from reserve boundaries. Essentially no difference in forest cover or forest loss is observed for the buffers 500–1000, 1000–1500, and 1500–3000 m from reserve boundaries.

Reserve level analysis of land-use and population change

Within the designated forest reserve areas, a total of 181 km^2 of forest transitioned to non-forest cover (i.e., open canopy and built) between circa 2003 and 2018. This represents a −4% decrease relative to the forest area mapped in circa 2003. Most of the reserves had a slight forest cover decrease during this period. Three reserves showed over −25% relative forest loss in circa 2018 when compared with the circa 2003 forest area, namely Anhwiaso North, Anhwiaso East, and Afoa Hills. These three reserves are located at the northwest end of the study area and have large-scale open pit mines nearby. Open pit

mines are mapped within Afao Hills for both study periods, with mining expansion during circa 2003–2018. A few reserves in the northeast of the mapping area showed a slight forest increase between circa 2003 and 2018. These include Aiyaola, Nsuensa, Bediako, and Mamang River Reserves. Despite being near mining activity, these reserves are also near large-scale plantation and commercial agriculture lands. When including the 1.5-km buffer region as reserve environs, eight reserves (including the three mentioned previously) had over −25% forest loss in circa 2018 compared with the forest area in circa 2003. All but one reserve is located in the western portion of the study area, and adjacent to mines. Kakum National Park showed a 0.6% increase in forest cover by circa 2018 compared with the circa 2003 forest area within the park boundary. The park and its environs combined exhibited a 2.98-km^2 increase in forest area or 1.3% during circa 2003–2018. Subri River, where large-scale forest clearing was observed from the classification maps, had a −11% relative forest decrease within the protected area during circa 2003–2018. This is likely due to forest plantation activity between planting and clear-cutting, as observed on the high spatial resolution reference images.

Figure 4 shows the scatterplots between population density change and forest cover change. The estimated population derived from the 2000 and 2010 censuses showed an increase in population for all the reserves (aggregated from EAs) and districts within the mapping area. As Fig. 4a shows, no significant correlation (R^2 = 0.05; $p = 0.1770$) was found between population density change and forest cover loss at the reserve level. Similar regression results were found when comparing population density of 2000 and 2010 with forest cover loss. Due to the limited availability of EA boundary

Table 2 Areal summary and change of forest, agriculture/open canopy, and built/bare/mining classes for the entire mapping area. The areal summary shows the area mapped for each class and the percentage relative to the mapping area. The areal change is calculated as the difference between image dates and percent change compared with the earlier date. Units are in km^2

Image date	Mapped area (km^2)		
	Forest	Open canopy	Built
c. 2003	6655 (68%)	3051 (31%)	70 (0.7%)
c. 2018	6030 (62%)	3586 (37%)	153 (1.6%)
2003–2018 change	− 625 (−9%)	535 (18%)	83 (119%)

Fig. 3 Land-cover and land-use change map between circa 2003 and 2018. The gray-scale background image is the NIR band of a Landsat 8 December 2015 image
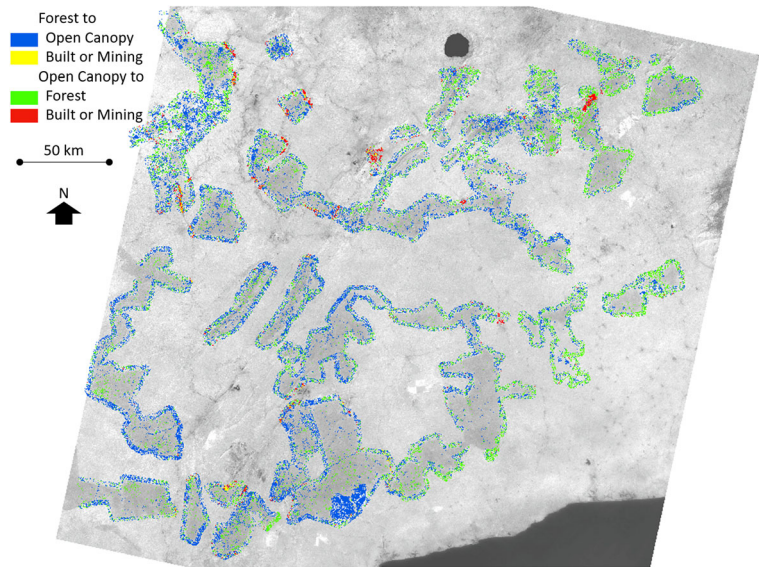
coverage, only the northern and eastern parts of the study area (a total of 38 reserves) were analyzed for the relationship between forest cover change and population gain. All the analyzed reserves showed a population increase and forest loss with varying degree. Annual population density change between 2000 and 2010 ranged from an increase of 1 to 14 people km^{-2} year^{-1}, with an average of 2 people km^{-2} year^{-1} (rural Ghana average population increase is about 1 person km^{-2} year^{-1}). The average relative forest cover loss between circa 2003 and 2018 per year is −1.3% and ranged from −0.4 to −2.3%. Ochi Headwaters forest reserve had the greatest increase in population density among the analyzed reserves, and also had a high relative forest loss at −37%. The Landsat-derived land-cover and land-use maps also indicated large-scale built expansion (from the town of Asin Foso) adjacent to both north and south ends of Ochi Headwaters. The reserve was established to protect the Ochi River water source

(Hawthorne and Abu-Juam 1995). Despite this goal, the Landsat-derived maps indicated drastic forest reduction from agriculture activity in the reserve. Anwiaso East reserve exhibited the greatest relative forest cover loss, with an average population density increase of 2 people km^{-2} year^{-1} (or a 6% annual increase) between 2000 and 2010. Kakum National Park area had a low population density increase at 1 person km^{-2}year^{-1} (12% annual increase).

District level analysis of land-use and population change

Table 4 shows the forest area mapped for circa 2003 and 2018 aggregated to the census district level, along with the population density for 2000 and 2010. Four out of the 14 districts showed forest cover increase, namely Ashanti Akim, Asikuma, Birim North, and Birim South. Birim North had the most forest increase of 29 km^2 or 15% compared with the forested area in 2003. These

Table 3 Areal summary of forest cover in relation to distance from reserve boundary. Forest loss is measured as the area that transitioned from forest in 2003 to non-forest in 2018, with the percentage showing the relative forest loss compared with forest in 2003

Distance from edge (m)	Total area (km^2)	2003 forest (km^2)	2018 forest (km^2)	Forest loss (km^2)
0–500	927	818 (88%)	762 (82%)	108 (13%)
500–1000	816	756 (93%)	728 (89%)	65 (9%)
1000–1500	680	634 (93%)	610 (90%)	53 (8%)
1500–3000	1145	1068 (93%)	1030 (90%)	87 (8%)
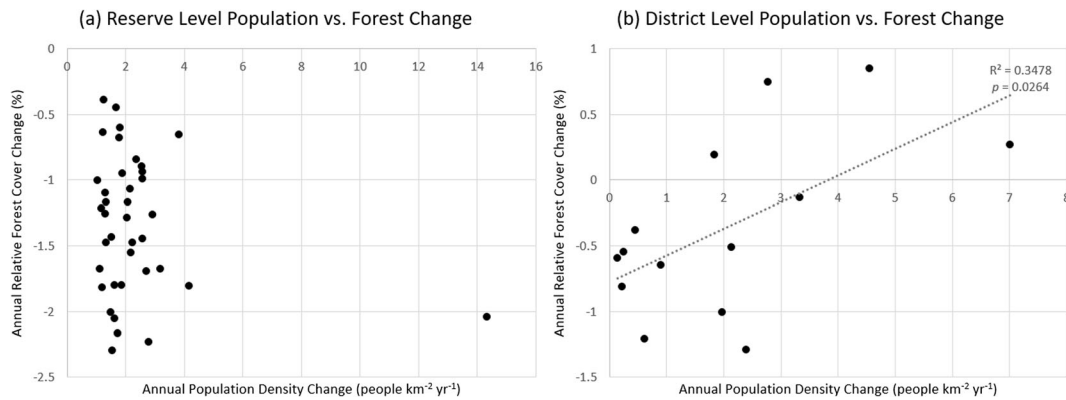
Fig. 4 Scatterplots of regression models for annual population density vs. forest cover change at the reserve level (**a**) and census district level (**b**). The annual population density was derived from the 2000 and 2010 censuses, and the annual relative forest cover change was measured based on the circa 2003 and 2018 Landsat-derived classification maps

four districts are located on the eastern side of the mapped area, as a north-south contiguous region. The remaining ten districts showed forest cover decreases,

Table 4 The mapped forest areal summary of 14 census districts for circa 2003 and 2018, and population density for 2000 and 2010 derived from the census data. The areal change is calculated as the difference between image dates and percent change compared with the earlier date. Units are in km^2. Population density is measured as the number of people per km^2 for a given district

District	Forest area (km^2)			Population density (people km^{-2})		
	2003	2018	Change	2003	2010	Change
Birim N.	189	218	+ 29 (15%)	107	152	45 (42%)
Asikuma	132	149	+ 17 (13%)	118	146	28 (24%)
Birim S.	306	320	+ 14 (5%)	143	213	70 (49%)
Ashanti Akim S.	183	189	+ 5 (3%)	83	101	18 (22%)
Assin	507	494	− 13 (− 3%)	93	126	33 (35%)
Twifu	386	359	− 27 (− 7%)	72	77	5 (7%)
Amansie E.	369	335	− 34 (− 9%)	113	134	21 (19%)
Nzema E.	366	330	− 36 (− 10%)	69	71	2 (3%)
Mpohor Wassa	869	776	− 93 (− 11%)	57	58	1 (2%)
Obuasi	608	537	− 71 (− 12%)	157	166	9 (6%)
Wassa Amenefi	1129	964	− 165 (− 15%)	49	51	2 (4%)
Amansie W.	211	173	− 38 (− 18%)	91	111	20 (22%)
Wassa W.	631	494	− 137 (− 22%)	86	92	6 (7%)
Bibiani	228	175	− 53 (− 23%)	124	148	24 (19%)

ranging from − 13 km^2 (Assin district) to − 165 km^2 (Wassa Amenefi). Percentage wise when comparing with the circa 2003 forest area, forest loss ranges from − 3 (Assin) to − 23% (Bibiani). Wassa Amenefi and Bibiani districts are adjacent to each other, located on the western edge of the study area. Assin district, where Kakum National Park is located, showed the least forest loss between 2003 and 2018.

At the district level, population density change between 2000 and 2010 showed a modest ($R^2 = 0.35$; $p = 0.0264$) inverse relationship with the amount of forest change between circa 2003 and 2018, as seen in Fig. 4b. On average, a 2-people-km^{-2} year $^{-1}$ increase was observed at the district level. In districts where there was forest reduction, population density showed a mild increase, ranging from a gain of 1 to 3 people km^{-2} year $^{-1}$. In districts where forest cover was mapped as an increase between circa 2003 and 2018, population density also showed greater increases. In the Bibiani district where forest cover reduced the most, annual population density change was average, at a 2-people-km^{-2} year $^{-1}$ increase. No correlation ($R^2 = 0.008$; $p = 0.8006$) was found between the annual population density change and the amount of forest cover loss when excluding the four districts of forest cover increase.

Discussion and conclusions

Land-use dynamics of over 70 forest reserves of tropical forest and the reserve environs were examined in this study. Dense Landsat image time series and median value SVVI composites were found effective in

minimizing the effects of no-data pixels due to cloud cover and yielded high classification accuracy in the cloud-prone southern Ghana area. The median value SVVI composites used in this study showed no residual clouds or other compositing artifacts, an improvement compared with the maximum-value composites used previously by Coulter et al. (2016). Some mapping confusion is apparent, as open canopy was mapped as closed forest for both image dates. Most misclassified pixels are associated with areas located outside of reserve boundaries, where secondary regeneration, plantation, and off-reserve forest could be confused with dense on-reserve forest cover. Available high spatial resolution imagery is limited for circa 2003, creating a challenge for generating reliable reference data for accuracy assessment. This could also lead to mapping disagreement and uncertainty, particularly between the open canopy and forest classes.

Land-cover and land-use change is most commonly associated with anthropogenic processes (IGBP report 1993; UNEP GEO-5 report 2012). In this study, anthropogenic activities such as mining, plantation/logging, agriculture, and built expansion were observed in southern Ghana from 1999 to 2018, resulting in declining forest cover and secondary regeneration/open canopy, even within protected areas. While subsistence farming and built expansion are the common and widespread threats to forest areas, other factors are more localized. Large-scale open pit mines expanded in a concentrated manner in the northwestern side of the study area (e.g., Anwhiaso) during circa 2003–2018. Although few mines are present within protected areas, drastic forest reduction is observed at both the reserve level and district level. While mining was also observed near reserves in the northeast of the study area, large-scale commercial agriculture/plantation is also present. Hawthorne and Abu-Juam (1995) documented logging activity and open canopy within these reserves, but observed concomitant forest regeneration. This may explain why extensive forest cover loss was not observed in the northeast region. Large-scale plantation activities such as afforestation and harvesting (when plantations mature) were observed in reserves within the southern part of the study region (e.g., Subri and Neung) as another source of land change. The commonly practiced taungya systems might increase human disturbances through additional subsistence agriculture activity within plantations in Ghana, leading to forest cover change and unsustainable forest management.

The livelihoods of rural households in Ghana depend heavily on forest-related income (Appiah et al. 2009; FAO 2016). While a growing rural population could mean an increasing reliance on forest resources, no correlation was found between the magnitude of forest and population change at the reserve level and a weak significant positive correlation at the district level in this study. The population density increase in the study area is relatively low with little variance, particularly at the reserve level (2 people km^{-2} $year^{-1}$). At the district level, the population data are summarized from a larger spatial extent than the mapped forest cover, such that populations included within census data do not necessarily reside or conduct activities near and within the reserves. Although percentage and density were used to standardize areal estimates, differences in area between the census and land-use analytical units likely influenced uncertainty in the regression analysis. More forest conservation efforts could also arise from scarce forest resources due to population increase (López-Carr and Burgdorfer 2013), resulting in less forest loss or even forest recovery. Deforestation has been associated with population growth in varying ways in other studies. Mertens and Lambin (2000) examined deforestation in South Cameroon with various potential land-cover and land-use change causes. They found that at the village level, deforestation is positively related to population growth while the highest magnitude of deforestation was found in villages with a small population. On the other hand, population density has been found to have an insignificant relationship with deforestation rate in the Brazilian Amazon (IGBP report 1993). DeFries et al. (2010) also found that tropical forest loss is not associated with rural population growth at a global scale. These varying results suggest that deforestation can be a complex type of land-cover and land-use change, and population alone might not be a sufficient predictor of forest loss (Lambin et al. 2001). Other factors such as affluence, land management policies, macro-economic factors, and political influences should also be considered in future studies.

Different types and magnitudes of land-cover and land-use changes were observed between protected and production reserves in this study. The only fully protected reserve found in the study area, Kakum National Park, exhibited minimal land-cover and land-use change, and relatively stable forest cover during the study periods. In addition to Kakum National Park, a cluster of reserves included in the Greater Kakum

working plans (including Assin and Pra Suhien) all showed stable forest cover between circa 2003 and 2018. Production reserves such as Subri River, Bowiye Range, and Opon Mansi each have a substantial plantation/productive area. These reserves all had over − 16% relative forest loss during circa 2003–2018 as mapped in the classification products. The variation suggests that reserve regulations and policies could be an influential factor in forest protection. However, we do not have the details of the working plans or the spatial extent of the production areas to quantitatively analyze forest change in different types of reserves for southern Ghana. Land management of protected areas is often defined locally in Ghana, because of the mostly private land ownership. Reserve management goals can vary from the protection of forests from logging and development, to protecting particular tree species, to protecting game and wildlife. Due to the variations in land ownership and management goals, a local or regional scale, such as the reserve and district levels used in this study, is appropriate for analyzing patterns of forest loss.

The data utilized in this study presented a few challenges, including Landsat and reference imagery availability, and census data quality. Few Landsat 4 and 5 TM images are available for the study area. We experimented with a circa 1991 composite image that yielded an overall forest mapping accuracy of 87%, while the forest in the northern portion of the map was commonly confused as open canopy and agriculture. A circa 2010 image composite generated from Landsat 7 images included scan line anomalies, especially in dense forest regions. The limited availability of high spatial resolution imagery as reference data led to higher uncertainty for accuracy assessment of land-cover and land-use change products. The mapped land-use changes were particularly difficult to verify, especially for the earlier study period of circa 2003. As an additional source of reference, we examined the Hansen Global Forest Change product (version 1.5; Hansen et al. 2013). The Hansen Change product indicated 1028 km^2 of forest loss in our mapping area between 2000 and 2017. This Change product defined forest as the biophysical tree coverage and excluded forest degradation (e.g., thinning) in the forest loss category. In our study, we mapped nearly 1500 km^2 of forest loss as land-cover type changes, and likely captured forest thinning as part of forest loss. The Hansen Change product and our change map depicted similar forest loss patterns in areas that showed forest clearing for mining, built-up land, and logging. Regarding the census data, EA boundaries were generated so that each delineated area contains similar populations. Following population increase, the EA boundaries were modified by the Ghana Statistical Services between the 2000 and 2010 censuses. Fortunately, because of the mostly rural mapping area, the discrepancies between the years were relatively minor. EA boundaries were ensured to share similar spatial extents. Because EA boundary files for 2010 are not completed for all of Ghana, the analysis of the population and forest change relationship was limited to the eastern portion of the study area, where the boundary files had been completed.

Google Earth Engine is open-access for education, research, and non-profit users. It provides an image library and a JavaScript coding platform for geospatial data analysis. Users can interactively implement and execute processes, and view results in an efficient manner utilizing its powerful cloud-based computing resources. The platform enabled dense time series of Landsat images to be processed, images to be composited, and unsupervised classification to be efficiently and effectively performed for this study, in just a few minutes. The image library eliminated the need for downloading a large quantity of imagery data. Compared with conventional image processing software, no license or installation is required for Earth Engine. The Earth Engine platform provides valuable resources for land-use and land-cover monitoring in a timely manner.

Monitoring forest resources for conservation and ecological purposes is critical, especially with the rapid population and economic growth of sub-Saharan Africa and Ghana. The mapping approach implemented on the cloud-based Google Earth Engine using the median value SVVI composite images was effective and efficient for monitoring forest cover and other land-use changes in the extremely cloud-prone southern Ghana. Other forested and cloud-prone regions could also benefit from this mapping approach. Future research should focus on exploring other anthropogenic factors that are potentially associated with deforestation to target management efforts. More frequent and extensive land-use monitoring could provide valuable information for government agencies to regulate and enforce logging and mining permits. Improved and updated land change estimates, as demonstrated with the mapping methods in this study, could also be used to support conservation efforts.

References

Acheampong, M., Yu, Q., Enomah, L. D., Anchang, J., & Eduful, M. (2018). Land use/cover change in Ghana's oil city: assessing the impact of neoliberal economic policies and implications for sustainable development goal number one–a remote sensing and GIS approach. *Land Use Policy, 73*, 373–384.

Appiah, M., Blay, D., Damnyag, L., Dwomoh, F. K., Pappinen, A., & Luukkanen, O. (2009). Dependence on forest resources and tropical deforestation in Ghana. *Environment, Development and Sustainability, 11*, 417–487.

Barraclough, S. L., & Ghimire, K. B. (2000). *Agricultural expansion and tropical deforestation: poverty, international trade, and land use*. London: Earthscan.

Broich, M., Hansen, M. C., Potapov, P., Adusei, B., Lindquist, E., & Stehman, S. V. (2011). Time-series analysis of multi-resolution optical imagery for quantifying forest cover loss in Sumatra and Kalimantan, Indonesia. *International Journal of Applied Earth Observation and Geoinformation, 13*(2), 277–291.

Calvo, C. M. (1994). *Case study on the role of women in rural transport: access of women to domestic facilities*. Washington, DC: World Bank.

Carr, D. L. (2004). Proximate population factors and deforestation in tropical agricultural frontiers. *Population and Environment, 25*(6), 585–612.

Carr, D. L., Suter, L., & Barbieri, A. (2005). Population dynamics and tropical deforestation: state of the debate and conceptual challenges. *Population and Environment, 27*(1), 89–113.

Coulter, L. L., Stow, D. A., Tsai, Y. H., Ibanez, N., Shih, H. C., Kerr, A., Bensa, M., Weeks, J. R., & Mensah, F. (2016). Classification and assessment of land cover and land use change in southern Ghana using dense stacks of Landsat 7 ETM+ imagery. *Remote Sensing of Environment, 184*, 396–409.

Debinski, D. M., Kindscher, K., & Jakubauskas, M. E. (1999). A remote sensing and GIS-based model of habitats and biodiversity in the Greater Yellowstone Ecosystem. *International Journal of Remote Sensing, 20*, 3281–3291.

DeFries, R. S., Rudel, T., Uriarte, M., & Hansen, M. (2010). Deforestation driven by urban population growth and agricultural trade in the twenty-first century. *Nature Geoscience, 3*(3), 178–181.

Dickson, K. B., Benneh, G., & Essah, R. R. (1988). *A new geography of Ghana*. London: Longman Publishing Group.

Foga, S., Scaramuzza, P. L., Guo, S., Zhu, Z., Dilley, R. D., Beckmann, T., Schmidt, G. L., Dwyer, J. L., Hughes, M. J., & Laue, B. (2017). Cloud detection algorithm comparison and validation for operational Landsat data products. *Remote Sensing of Environment, 194*, 379–390.

Food and Agriculture Organization (FAO) of the United Nations. (2016). *State of the world's forest 2016*. Rome: FAO.

Franklin, S. E., & Wulder, M. A. (2002). Remote sensing methods in medium spatial resolution satellite data land cover classification of large areas. *Progress in Physical Geography, 26*(2), 173–205.

Ghana Statistical Service. (2012). *2010 population & housing census summary report of final results*. Accra: Ghana Statistical Service.

Hall, J. B., & Swaine, M. D. (1976). Classification and ecology of closed-canopy forest in Ghana. *Journal of Ecology, 64*(3), 913–951.

Hall, F., Strebel, D., Nickeson, J., & Goetz, S. (1991). Radiometric rectification: toward a common radiometric response among multidate, multisensor images. *Remote Sensing of Environment, 35*, 11–27.

Hansen, M. C., Roy, D. P., Lindquist, E., Adusei, B., Justice, C. O., & Altstatt, A. (2008). A method for integrating MODIS and Landsat data for systematic monitoring of forest cover and change in the Congo Basin. *Remote Sensing of Environment, 112*(5), 2495–2513.

Hansen, M. C., Potapov, P. V., Moore, R., Hancher, M., Turubanova, S. A. A., Tyukavina, A., Thau, D., Stehman, S. V., Goetz, S. J., Loveland, T. R., & Kommareddy, A. (2013). High-resolution global maps of 21st-century forest cover change. *Science, 342*(6160), 850–853.

Hawthorne, W. D., & Abu-Juam, M. (1995). *Forest protection in Ghana*. Gland: IUCN.

Hens, L., & Boon, E. K. (1999). Institutional, legal, and economic instruments in Ghana's environmental policy. *Environmental Management, 24*(3), 337–351.

Hilson, G., & Nyame, F. (2006). Gold mining in Ghana's forest reserves: a report on the current debate. *Area, 38*(2), 175–185.

Huang, C., Goward, S. N., Masek, J. G., Gao, F., Vermote, E. F., Thomas, N., Schleeweis, K., Kennedy, R. E., Zhu, Z., Eidenshink, J. C., & Townshend, J. R. (2009). Development of time series stacks of Landsat images for reconstructing forest disturbance history. *International Journal of Digital Earth, 2*(3), 195–218.

International Geosphere-Biosphere Programme (IGBP), 1993. Relating land use and global land-cover change: a proposal for an IGBP-HDP core project. Stockholm.

Kalame, F. B., Aidoo, R., Nkem, J., Ajayie, O. C., Kanninen, M., Luukkanen, O., & Idinoba, M. (2011). Modified taungya system in Ghana: a win–win practice for forestry and adaptation to climate change? *Environmental Science & Policy, 14*(5), 519–530.

Kusimi, J. M. (2008). Assessing land use and land cover change in the Wassa West District of Ghana using remote sensing. *GeoJournal, 71*(4), 249–259.

Lambin, E. F., Turner, B. L., Geist, H. J., Agbola, S. B., Angelsen, A., Bruce, J. W., Coomes, O. T., Dirzo, R., Fischer, G., Folke, C., & George, P. (2001). The causes of land-use and land-cover change: moving beyond the myths. *Global Environmental Change, 11*(4), 261–269.

Lindquist, E. J., Hansen, M. C., Roy, D. P., & Justice, C. O. (2008). The suitability of decadal image data sets for mapping tropical forest cover change in the Democratic Republic of Congo: implications for the global land survey. *International Journal of Remote Sensing, 29*(24), 7269–7275.

López-Carr, D., & Burgdorfer, J. (2013). Deforestation drivers: population, migration, and tropical land use. *Environment: Science and Policy for Sustainable Development, 55*(1), 3–11.

Masek, J. G., Vermote, E. F., Saleous, N. E., Wolfe, R., Hall, F. G., Huemmrich, K. F., Gao, F., Kutler, J., & Lim, T. K. (2006). A Landsat surface reflectance dataset for North America, 1990-2000. *IEEE Geoscience and Remote Sensing Letters, 3*, 68–72.

Mertens, B., & Lambin, E. F. (2000). Land-cover-change trajectories in southern Cameroon. *Annals of the American Association of Geographers, 90*(3), 467–494.

Moran, M. S., Jackson, R. D., Slater, P. N., & Teillet, P. M. (1992). Evaluation of simplified procedures for retrieval of land surface reflectance factors from satellite sensor output. *Remote Sensing of Environment, 41*, 169–184.

Muller, S. V., Racoviteanu, A. E., & Walker, D. A. (1999). Landsat MSS-derived land-cover map of northern Alaska: extrapolation methods and a comparison with photo-interpreted and AVHRR-derived maps. *International Journal of Remote Sensing, 20*, 2921–2946.

Murcia, C. (1995). Edge effects in fragmented forests: implications for conservation. *Trends in Ecology & Evolution 10* (2): 58–62

Osafo, Y. B. (2005). *Reducing emissions from tropical forest deforestation: applying compensated reduction in Ghana* (p. 6372). Tropical Deforestation and Climate Change.

Pabi, O. (2007). Understanding land-use/cover change process for land and environmental resources use management policy in Ghana. *GeoJournal, 68*(4), 369–383.

Planet Team and Planet Application Program Interface: In space for life on earth. San Francisco, CA. 2017 URL https://api.planet.com (accessed on August 2018).

Rogan, J., & Chen, D. (2004). Remote sensing technology for mapping and monitoring land-cover and land-use change. *Progress in Planning, 61*(4), 301–325.

Roy, D. P., Wulder, M. A., Loveland, T. R., Woodcock, C. E., Allen, R. G., Anderson, M. C., Helder, D., Irons, J. R., Johnson, D. M., Kennedy, R., & Scambos, T. A. (2014). Landsat-8: science and product vision for terrestrial global change research. *Remote Sensing of Environment, 145*, 154–172.

Ruefenacht, B. (2016). Comparison of three Landsat TM compositing methods: a case study using modeled tree canopy cover. *Photogrammetric Engineering and Remote Sensing, 82*(3), 199–211.

Ubink, J. M., & Quan, J. F. (2008). How to combine tradition and modernity? Regulating customary land management in Ghana. *Land Use Policy, 25*(2), 198–213.

United Nations, 2010. The world's women 2010: trends and statistics. United Nations, New York.

United Nations, Department of Economic and Social Affairs (UN DESA), 2017. 2016 international trade statistics yearbook. United Nations, New York.

United Nations, Department of Economic and Social Affairs (UN DESA), 2018. 2018 revision of world urbanization prospects. United Nations, New York.

United Nations Educational, Scientific and Cultural Organization (UNESCO). (1973). *International classification and mapping of vegetation*. Paris: UNESCO.

United Nations Environment Programme (UNEP). (2012). *Global Environmet Outlook Report (GEO-5) Chapter 3: Land*. Nairobi: UNEP.

Vermote, E., Justice, C., Claverie, M., & Franch, B. (2016). Preliminary analysis of the performance of the Landsat 8/OLI land surface reflectance product. *Remote Sensing of Environment, 185*, 46–56.

Wu, C. (2004). Normalized spectral mixture analysis for monitoring urban composition using ETM+ imagery. *Remote Sensing of Environment, 93*, 480–492.

Yorke, C., & Margai, F. M. (2007). Monitoring land use change in the Densu River basin, Ghana using GIS and remote sensing methods. *African Geographical Review, 26*(1), 87–110.